Aditya V. Yalamanchili
Department of Mechanical Engineering,
Texas A&M University,
College Station, TX 77840
email: yadityavarma@tamu.edu

Dinakar Sagapuram
Department of Industrial and Systems Engineering,
Texas A&M University,
College Station, TX 77843
email: dinakar@tamu.edu

Prabhakar R. Pagilla[1]
Department of Mechanical Engineering,
Texas A&M University,
College Station, TX 77840
email: ppagilla@tamu.edu

Modeling and control of strip transport in metal peeling

Metal peeling refers to the process of forming a thin metal strip from the surface of a rotating feedstock using controlled material removal – machining under an applied strip tension. In this paper,the mechanics of strip formation process is described, while emphasizing the role of strip tension in ensuring uniformity and quality of the peeled strip. This includes an analysis of the deformation history in the peeling zone and the transport dynamics of the strip as it moves from the cutting edge to the coiler. Using conservation laws, governing equations for strip tension and velocity that incorporate dynamic spatiotemporal interactions between peeling and transport processes are developed.Experimental demonstration includes the setup of a lab-scale prototype metal peeling system designed to validate the proposed dynamic model describing the strip transport behavior and control approach. Peeling experiments are performed with steel using a prototype experimental platform to evaluate the proposed control approach. Comparisons between two control strategies, with and without tension feedback, are presented and discussed. The importance of real-time tension control for mitigating strip thickness variations and improving other dimensional features of the strip such as flatness and edge waviness is also briefly discussed.

Keywords: Modeling, dynamic behavior, real-time control, metal peeling, strip manufacturing

1 INTRODUCTION

Industrial production of metal coils in strip and sheet form[2] is driven by hot and cold rolling processes where a rectangular cast slab is progressively reduced in its thickness in multiple deformation passes. The process of transforming the cast material into final coil product includes multiple heating, cooling, annealing and finishing steps between the rolling passes to relieve stresses, prevent material from cracking, and achieve the desired microstructure and properties [1]. Although mature, metal strip and sheet production using rolling is intrinsically energy intensive. Specifically in the cases of steels, it also contributes to significant carbon emissions due to the need for heating the metal to high temperatures (in excess of 1,000°C) during hot rolling [2,3].

Metal peeling is an energy efficient alternative to rolling where a thin continuous strip is produced directly from a rotating solid metal feedstock via cutting (machining) action of a sharp tool, see Fig. 1. The primary advantage of this process is that thin metal strip is practically produced in a single step, thus eliminating the need for multiple deformation passes and intermediate processing steps intrinsic to traditional rolling. Moreover, because only a small localized material volume in the vicinity of the cutting edge is subjected to deformation at any time instance, the need for preheating the metal to high temperatures is also eliminated. Lastly, the energy footprint of the process is nearly independent of the strip thickness, whereas in rolling, both energy consumption (per unit volume) and processing steps increase exponentially with decreasing strip thickness. This makes metal peeling especially attractive for production of strips with finer gauges (e.g., foil thicknesses).

The concept of peeling as a means to produce thin metal strip has been known for nearly a century, dating back to Junker [4]. The technology has since witnessed several innovations and refinements both

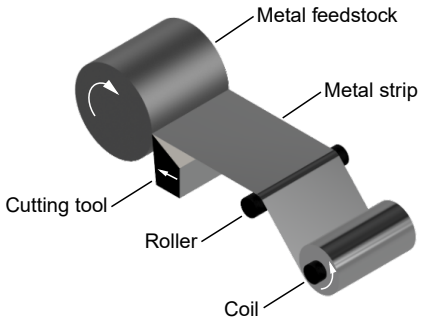

Fig. 1 Sheet metal production by metal peeling.

in terms of methods of practice and machine design [5–7]. These subsequent studies have shown that by combining peeling with a take-up coiler, the process can be operated continuously to produce metal coils with properties comparable to that of strip manufactured conventionally. In such a configuration, the key components of the peeling system include: (1) a spindle that rotates the feedstock, typically at a constant surface velocity; (2) a cutting tool assembly that feeds the cutting edge along the radial direction of the rotating feedstock at a constant feed per revolution; and (3) a downstream strip transport system that collects and coils the strip, while often applying a slight "pull" on the incoming strip.

A significant challenge in strip production by peeling is the control of strip thickness. Unlike rolling where strip thickness is determined by the roller-gap setting, strip thickness in peeling is not controlled *a priori* but is an output of the process that is influenced by various factors including feedstock properties, cutting tool edge condition and peeling process parameters. Any changes in these variables during the process may thus induce thickness variations along the length of the strip. Two methods that were previously proposed to control strip thickness and potential variations with time include: (1) regulation of coiler surface velocity at a value that remains constant with respect to feedstock surface velocity, and (2) regulation of back tension that is applied on the strip during peeling. Thickness control via regulation of coiler velocity for instance

[1]Corresponding Author.
September 16, 2024

[2]The terms *sheet*, *strip* and *foil* are used in the industry to distinguish flat rolled products based on their thickness and width. For instance, according to the ASTM A480 specification for steels, flat rolled steel sheet is categorized as a material with a thickness less than 5 mm and a width equal to or exceeding 600 mm. In contrast, strip steel is identified as material with a width less than 600 mm. Foil is defined as a metal strip with a thickness less than 0.15 mm, and foils having a narrow width are referred to as "ribbons".

involved the use of a speed sensor to measure the transport velocity of the peeled strip and subsequently adjusting the coiler rotational speed to achieve and maintain a desired strip thickness [6,8]. This is analogous to flexible material (web) transport by speed regulation in roll-to-roll processing systems. Another speed-based thickness control method involved maintaining a fixed ratio between the peripheral velocities of the feedstock and the coiler by formulating a time-based relationship [9]; this method has the advantage that it does not need in-line measurement of strip thickness. However, a drawback of these speed-based control systems is the lack of direct information about the tension that develops in the strip; this is important since excessive tensile stresses in the strip may result in material failure due to plastic yielding and necking [10]. Thickness control via tension regulation overcomes this problem and is based on the experimental observation that the thickness at which the strip forms at the cutting edge is influenced by the level of tension applied on the strip and the pulling angle. Therefore, strip thickness can be controlled and maintained constant by controlling the tension and pulling angle, as long as the feedstock properties do not change substantially from beginning to the end of the peeling process. In the control mechanism developed by Brown [7], the constant tension in the strip was achieved by continuously adjusting the torque at the coiler. Interestingly, this mechanism also included an option for simultaneously altering the tool feed rate to account for any variations in the feedstock metallurgical state such that both thickness and tension are concurrently maintained constant.

A variant of the peeling technique that should be mentioned is a process referred to as extrusion-machining [11–14]. In this process, a secondary tool, referred to as the constraint, is placed directly opposite to the primary cutting tool to create a die opening so that peeling (machining) and extrusion occur simultaneously. This converts peeling into a geometrically well-defined deformation process, where the thickness of the peeled strip is fully determined *a priori* by the gap between the cutting tool and the constraint edge. While the constrained peeling technique offers improved control of strip thickness, in continuous coil production, the ability to control back tension on the strip is still desirable since application of tension during peeling (either free or constrained) even at stresses much below the material's yield strength has been known to significantly improve strip flatness, straightness (camber) and thickness uniformity across the width [15].

In continuous manufacturing applications such as roll-to-roll (R2R) manufacturing, it is customary to start with a model for the material transport and develop corresponding governing equations that can be used as a basis for developing informed control systems. Over the past few decades, significant strides have been made in the development of mathematical models for transport of webs (metals and otherwise) in R2R processing systems, see [16–21]. While the general theoretical framework in all cases is based on the common balance laws, each R2R application necessitates tailored consideration of the material's mechanical behavior and the process associated with transporting the web since both impact the transport dynamics. In the case of metal peeling, a significant challenge lies in addressing the interaction between applied tension and strip thickness; for example, any temporal changes in tension during peeling are reflected as spatial variations in strip thickness along the coil. This is different from typical R2R applications where the web thickness is assumed to remain constant within a given span unaffected by the transport dynamics but is somewhat similar to the situation in in tandem and reversible rolling mills where transport tension can induce plastic deformation in the strip and thereby impacts the strip cross-section (thickness). In this regard, recent advancements in control strategies for metal processing include employing Lyapunov methods [22] and receding horizon control [23]. Specifically in the case of reversible col rolling of metals, control strategies utilizing adaptive backstepping [24] and Hamilton-based adaptive robust control [25] have been developed. In [26], several control approaches for looper and tension control in hot strip mills, including PID, sliding mode control and linear quadratic regulators are also discussed.

This paper describes a study that was undertaken to develop a model for strip transport in metal peeling, and corresponding governing equations for strip tension, thickness and velocity. To the best of our knowledge, there is no existing literature on this particular topic. Based on this model, a closed-loop control approach is presented for regulating strip tension (thereby thickness and velocity) and the efficacy of the control strategy is demonstrated using a prototype peeling system developed to conduct controlled peeling, transport and coiling experiments with steels. The positive effect of tension on strip thickness uniformity and dimensional quality is also discussed.

2 STRIP FORMATION PROCESS IN PEELING

Strip production by peeling involves continuously removing a thin layer of material from the surface of a rotating feedstock by feeding a sharp cutting tool edge at a constant rate (mm/rev). This process may be effectively understood by studying the continuous chip formation process in orthogonal cutting [27], see Fig. 2. In orthogonal cutting, the cutting edge of the tool is perpendicular to the direction of the tool feed motion and when the width of the cut (w) is large compared to the depth of cut (t_0), the process can be approximated as one of plane-strain, i.e., negligible material flow along the width direction. The type of chip (strip) that forms in orthogonal cutting is sensitive to both feedstock properties and cutting process conditions [28]. When cutting ductile metals such as steels, copper and aluminum alloys under moderate cutting speeds (< 5 m/s), a continuous strip with a uniform thickness is generally produced. Under these conditions, the material flow and plastic deformation during cutting is often modeled using shear plane (or shear zone) models [29–31]. In this picture, the transformation of feedstock material into deformed chip is considered to take place via steady-state plastic shear along a thin shear plane or zone (AB in Fig. 2). The shear is such that it results in a strip thickness (t_s) that is almost always greater than the depth of cut (t_0). A quantity of interest here is the chip thickness ratio, $r = t_0/t_s$; for instance, in steels, r is typically in the 0.3-0.5 range. If v_0 is the surface velocity of the feedstock and v_1 is the exit strip velocity, the law of conservation of mass (assuming constant density and plane-strain deformation) dictates that

$$r = \frac{t_0}{t_s} = \frac{v_1}{v_0}. \tag{1}$$

An important distinction between conventional orthogonal cutting and peeling is that in the latter, the strip is formed under simultaneous action of a pulling force (tension) that is applied either along the cutting tool face or at some angle to it. That this application of tension on the strip while it is being peeled has a substantial effect on both the strip thickness and curl has been well-known in the literature, although the exact mechanism(s) by which tension effects come about is not well-understood. For instance, Nakayama's experiments [32] with copper have shown that applying tension can result in large reductions in strip thickness and the cutting force, by up to one-half and one-third of their original values (i.e., without tension). Referring to Fig. 2, this means that the thinner strip under

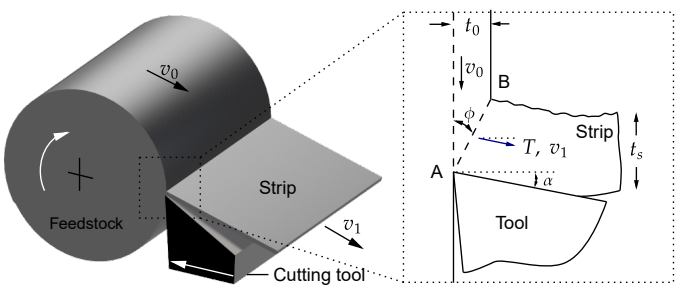

Fig. 2 Schematic of peeling process, with the inset showing peeling variables and strip geometry.

tension forms at a larger shear angle (ϕ) with respect to the v_0 direction. Subsequent work by Walters and Childs [10,33] has shown that the strip thickness dependence on applied tension is monotonic, showing a steady decrease with increasing tension until interrupted by material failure (strip breakage) when the tensile stresses reach close to the strip material's shear flow stress $\sim \sigma_y/2$. The effect of tension on strip thickness was also shown to be more pronounced when the pull was applied at a 20-30° angle as opposed to parallel to the cutting tool face. It should be noted that the deformation geometry in cutting, determined by the ratio r, also governs the level of plastic strain and material strain hardening at the shear zone. More specifically, for a given t_0, plastic strain decreases with increasing r or decreasing t_s. Therefore, strips produced under tension having a larger r value are generally more malleable compared to those produced by free cutting (zero tension, smaller r) that tend to be rather brittle. Thus, the ability to control tension during peeling is not only critical for controlling strip thickness but also for producing a ductile strip with improved dimensional properties (including reduced curl and camber).

For developing a tension controller, it is desirable to have a model that allows prediction of strip geometry (thickness and curl) as a function of applied tension and pulling angle. However, analytical prediction of these quantities even for conventional cutting without tension is a considerable challenge, due to the extreme strain and strain rate conditions intrinsic to cutting and the lack of well-defined boundary conditions at the tool-chip contact, see discussion in [28,34–37]. While finite element simulations can be used to model the relevant phenomena with high accuracy, their computational complexity and time-intensive nature make them less suitable for direct implementation into real-time controllers. In this study, we build on previous experimental literature on strip peeling under tension, specifically Nakayama [32], Walters and Childs [10,33] and Finnie [38], which suggests a monotonic decrease in strip thickness with tension for a given pulling angle. This empirical observation is central to the strip transport model presented in this paper to model the dynamic behavior of strip tension, thickness and velocity.

3 MODELING OF PEELED STRIP TRANSPORT

3.1 Deformation history in peeling. The mechanics of strip formation and subsequent transport under tension is modeled in the following manner. Consider the example of a material exhibiting elastic-plastic (strain hardening) behavior. For an arbitrary material point with the pathline PQRS in Fig. 3(*a*), the corresponding equivalent (von Mises) stress state is depicted in Fig. 3(*b*). The plastic deformation begins when the equivalent stress reaches the material yield strength, σ_y (at Q), and continues through the shear zone (Q to R) where the material undergoes strain hardening. Upon exiting the shear zone, the material point experiences unloading. However, instead of stress dropping to zero, it reduces to a finite σ_s in the elastic regime, where σ_s is the uniaxial tensile stress due to strip tension. The stress due to tension is assumed to be uniformly distributed across the cross-section of the strip and that every point in the peeled strip is subjected to the same applied tension. As a reference, point U (see Fig. 3(*b*)) denotes the stress-free configuration (unstretched state) of the strip. If we denote the total strain at S by ε_t and the plastic strain imposed in the shear zone by ε_p, then the elastic strain is given by: $\varepsilon = \varepsilon_t - \varepsilon_p$. Note also that the plastic strain in the strip itself depends on tension. For example, if the strip is peeled with a different applied tension and correspondingly different stress $\sigma_s' > \sigma_s$, then the same material point entering the shear zone at Q would exit the plastic deformation zone at R' with a lower plastic strain, but continues to carry a higher elastic strain component.

The governing equation for strip tension in the span immediately downstream of the peeling process is derived by using the law of conservation of mass applied to a control volume defined by the strip span between the shear zone (AB) and the coiler, see Fig. 4. The following assumptions are made in this derivation: (1) strip transport is purely elastic, i.e., after exiting the shear zone the material experiences only recoverable elastic deformations; (2) the idle rollers (including load cell roller) are frictionless and do not contribute to the strip tension dynamics during steady-state operation; (3) width of the peeled strip is the same as that of the feedstock (i.e., plane-strain deformation) and the mass entering the shear zone is equal to the mass exiting to form the peeled strip at any given time; (4) density changes during strip formation and transport are negligible; and (5) elastic strains during strip transport are small compared to the plastic strains. The last assumption is based on the fact that σ_s is typically a small fraction of σ_y and since σ_y/E ratio for metals is in the order of 10^{-3} to 10^{-2}, the resulting elastic strains are quite small compared to the plastic strains.

3.2 Strip transport dynamics. Application of the conservation of mass for the control volume (Fig. 4) gives the following relation:

$$\frac{d}{dt}\left[\int_0^L \rho(x,t)A(x,t)dx\right] = \rho_1(t)A_1(t)v_1(t) - \rho_2(t)A_2(t)v_2(t), \qquad (2)$$

where L is the length of the strip span between the cutting edge and the coiler, ρ is the material density, A is cross-sectional area of the peeled strip, v_i is the transport velocity, x is the transport direction and t is time. Indices $i = 0, 1, 2$ represent the feedstock, span entry and span exit/coiler respectively. Additionally, the following notation is used: T, strip tension; w, strip width; t_s, peeled strip thickness under tension T; t_0, depth of cut; E_s, modulus of elasticity of the strip; E_f, modulus of elasticity of the feedstock; ε_x, ε_y, and ε_z, the elastic strains in x (transport), y (thickness), and z (lateral) directions, respectively.

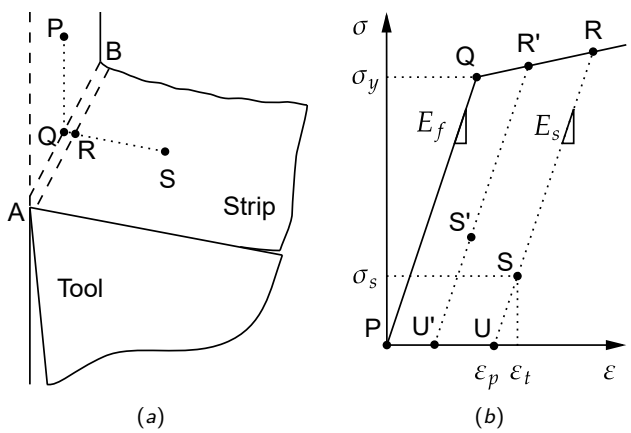

Fig. 3 Pathline (a) and the corresponding stress history (b) of an arbitrary material point passing through the shear zone (AB).

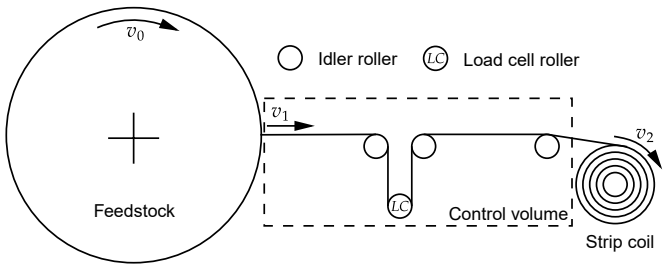

Fig. 4 Illustration of strip transport from the peeling edge to the coiler. The control volume is shown using the dashed box.

For a representative strip elemental mass dm, application of mass balance gives

$$dm = \rho w t_s dx = \rho_u w_u t_u dx_u, \tag{3}$$

where dx denotes the length of the elemental mass dm, and the subscript u represents the unstretched state; for example, t_u denotes the stress-free strip thickness in the state U in Fig. 3(*b*). The relationships between the stretched and unstretched dimensions are given by:

$$dx = (1 + \varepsilon_x)\, dx_u, \tag{4a}$$

$$t_s = \left(1 + \varepsilon_y\right) t_u, \tag{4b}$$

$$w = (1 + \varepsilon_z)\, w_u. \tag{4c}$$

Combining (3) and (4a) gives

$$\frac{\rho w t_s}{\rho_u w_u t_u} = \frac{dx_u}{dx} = \frac{1}{1 + \varepsilon_x}. \tag{5}$$

Applying mass balance across the shear zone AB (Fig. 3(*a*)) and using the assumption (3), it follows that

$$\rho_1 w_1 t_{s1}(t) v_1(t) = \rho_0 w_u t_0 v_0. \tag{6}$$

Noting that $A(x,t) = w t_s(x,t)$, and substituting (5) and (6) in (2) gives

$$\frac{d}{dt}\left[\int_0^L \frac{\rho_u(x,t) w_u t_u(x,t)}{1 + \varepsilon_x(x,t)} dx\right] = \rho_0 w_u v_0 t_0 - \frac{\rho_{2u}(t) w_u t_{u2}(t)}{1 + \varepsilon_{x2}(t)} v_2(t), \tag{7}$$

where the subscripts 1 and 2 on the variables denote their values at span locations $x = 0$ and $x = L$, respectively. Equation (7) may be further simplified using assumption (4) to

$$\frac{d}{dt}\left[\int_0^L \frac{t_u(x,t)}{1 + \varepsilon_x(x,t)} dx\right] = v_0 t_0 - \frac{t_{u2}(t)\, v_2(t)}{1 + \varepsilon_{x2}(t)}. \tag{8}$$

Using the small strain assumption (5), i.e., $\varepsilon << 1$, a further simplification can be made: $1/(1+\varepsilon) \approx (1 - \varepsilon)$. Therefore,

$$\frac{d}{dt}\left[\int_0^L \left(1 - \varepsilon_x(x,t)\right) t_u(x,t) dx\right] = v_0 t_0 - \left(1 - \varepsilon_{x2}(t)\right) t_{u2}(t) v_2(t). \tag{9}$$

Let $\varepsilon_x^m(x,t)$ denote the mechanical strain due to strip tension and $\varepsilon_x^\theta(x,t)$ denote the thermal strain due to temperature rise. The total strain in the peeled strip is given by [39,40]

$$\varepsilon_x(x,t) = \varepsilon_x^m(x,t) + \varepsilon_x^\theta(x,t). \tag{10}$$

The mechanical and thermal strains are given by

$$\varepsilon_x^m(x,t) = \frac{T(t)}{w_u t_u(x,t) E_s(x)}, \tag{11a}$$

$$\varepsilon_x^\theta(x) = \alpha_\theta \left[\theta(x) - \theta_\infty\right], \tag{11b}$$

where α_θ is the coefficient of thermal expansion of the material, $\theta(x)$ is the temperature of the strip, θ_∞ is the ambient temperature, and $E_s(x)$ is a function of the strip temperature. Steady-state temperature and thermal strain in the strip are time independent, and thus depend only on the spatial coordinate x. Substituting for the strains in (9) gives

$$\frac{d}{dt}\left[\int_0^L \left(1 - \varepsilon_x^m(x,t) - \varepsilon_x^\theta(x)\right) t_u(x,t) dx\right] = v_o t_0 - \left(1 - \varepsilon_2^m(t) - \varepsilon_2^\theta\right) t_{u2}(t) v_2(t), \tag{12}$$

where $\varepsilon_2^m = \varepsilon_x^m(L,t)$, $\varepsilon_2^\theta = \varepsilon_x^\theta(L)$. Equation (12) is a general form of the governing equation for strip transport in metal peeling, which may be further simplified under special scenarios to facilitate further analysis and development of a control law.

The relationship between the thickness t_{u1} and the peeling process conditions can be represented using

$$t_{u1} = \frac{t_0}{r(T, v_0, \alpha, \ldots)}. \tag{13}$$

Under constant cutting parameters (t_0, v_0 and α) and operating tension reference T_r, the change in the strip thickness, $\widetilde{t}_{u1}(t)$ may be approximated (using a first order Taylor series expansion) as linearly varying with the change in strip tension, $\widetilde{T}(t) := T(t) - T_r$, as follows:

$$t_{u1}(t) = t_r - k\widetilde{T}(t), \tag{14}$$

where t_r is the reference (desired) strip thickness when peeled under tension T_r, $\widetilde{T}(t) = T(t) - T_r$ is the tension error, $k = -\left.\frac{\partial t_{u1}}{\partial T}\right|_{T=T_r}$, and $k > 0$. Further, the longitudinal variation in the strip thickness (transport lag) in the span may be expressed as:

$$t_u(x,t) = t_{u1}(t - \tau(x)), \quad \text{where} \quad \tau(x) = \frac{x}{v(x)}, \tag{15}$$

and $v(x)$ is the strip transport velocity that changes from v_1 at $x = 0$ to v_2 at $x = L$. Note that the above transport lag equation means that once the strip is formed with a certain thickness at peeling ($x = 0$), then this thickness does not change during transport through the span. Let v_{2r} denote the reference strip transport velocity at tension T_r. Since the strip velocity variations in the span are small, for the purpose of computing transport lag $\tau(x)$, it is assumed that $v(x) = v_{2r}$. Combining (14) and (15) gives the following relationship for the spatial variations in strip thickness in the span due to temporal changes in tension

$$t_u(x,t) = t_r - k\widetilde{T}(t - x/v_{2r}). \tag{16}$$

Note that strip formation by peeling is a mechanical process where large plastic deformation in the shear zone and frictional dissipation at the tool-chip contact under high strain rates can cause significant local temperature rise near the peeling edge. However, the use of flood lubrication (a common practice in metal cutting), coupled with thin strip cross-sections result in rapid cooling of the strip to ambient temperature levels in a time span (~500 ms) that is much smaller compared to the characteristic time-scale ($\sim L/v$) associated with strip transport in the span. Thus, for the current purpose, thermal strains are neglected in the study. Consequently, the modulus is independent of temperature and the spatial coordinate, i.e., $E_s(x) \approx E_f \approx E$. Thus, (12) can be simplified to

$$\frac{d}{dt}\left[\int_0^L \left(t_u(x,t) - t_u(x,t)\varepsilon_x^m(x,t)\right) dx\right] = v_0 t_0 - t_{u2}(t) v_2(t) + t_{u2}(t) v_2(t) \varepsilon_2^m(t). \tag{17}$$

Substituting the mechanical strain given by (11a) and the thickness transport lag equation given by (16) into above equation gives

$$\frac{d}{dt}\left[\int_0^L t_u(x,t)dx\right] - \eta\dot{T}(t)$$

$$= v_0 t_0 - \left(t_r - k\widetilde{T}(t-\tau_2)\right)v_2(t) + \frac{\eta T(t)}{L}v_2(t), \tag{18}$$

where $\eta = L/(w_u E)$ and $\tau_2 = \tau(L)$. The time derivative of the definite integral in the above equation is evaluated by substituting $t_u(x,t)$ from (16) and using the Leibniz integral rule and the fundamental theorem of calculus. It follows that

$$\frac{d}{dt}\left[\int_0^L t_u(x,t)dx\right] = -v_{2r}k\left(\widetilde{T}(t) - \widetilde{T}(t - L/v_{2r})\right). \tag{19}$$

A similar approach was employed in [41] to derive the tension governing equation for spans with time-varying length. Substituting (19) in (18) gives

$$\eta\dot{T}(t) = \left(t_r - k\widetilde{T}(t-\tau_2)\right)v_2 - t_0 v_0$$

$$- v_{2r}k\left(\widetilde{T}(t) - \widetilde{T}(t-\tau_2)\right) - \frac{\eta T(t)}{L}v_2(t). \tag{20}$$

Equation (20) represents the nonlinear governing equation for strip tension in metal peeling; note that this governing equation is different from those obtained for transport of ordinary webs with constant thickness in traditional unwind/rewind roll-to-roll systems.

3.3 Coiler dynamics. The dynamics of the coiler with time varying inertia is given by [20]

$$\frac{J_2(t)}{R_2(t)}\dot{v}_2(t) = -T(t)R_2(t) + n_2 u_2(t) - \frac{b_{f2}}{R_2(t)}v_2(t)$$

$$+ \frac{t_{s2}(t)}{2\pi R_2}\left(\frac{J_2(t)}{R_2^2(t)} - 2\pi\rho w R_2^2(t)\right)v_2^2(t), \tag{21}$$

where J_2 is the effective inertia of the coiler, n_2 is the gearing ratio between the motor shaft and coiler roll shaft, R_2 is the radius of the coil, b_{f2} is the coefficient of friction in the coiler roll shaft, and u_2 is the input torque to the motor. Assuming that the radius of the coil is slowly time-varying, i.e., the coil buildup is very slow at small transport velocities ($\dot{R}_2 \approx 0$), the dynamics of the coiler is simplified to

$$\frac{J_2}{R_2}\dot{v}_2(t) = -T(t)R_2 + n_2 u_2(t) - \frac{b_{f2}}{R_2}v_2(t). \tag{22}$$

Equations (20) and (22) together represent a control-oriented model for strip transport dynamics in metal peeling that incorporates key physical phenomena and coupling between tension, thickness and transport velocity.

4 CONTROL DESIGN

The primary control objective is to regulate strip tension and transport velocity (since they are coupled, as evident from the governing equations) to ensure uniformity of the peeled strip thickness and efficiency of the peeling, transport and coiling processes. To achieve this objective, the control problem can be posed as follows. Given the strip material and coiler parameters, feedstock surface velocity v_0, depth of cut t_0, reference thickness t_r, and reference tension T_r: (1) determine the reference velocity of the coiler (v_{2r}) and the equilibrium or feedforward control input (u_{2r}) required to maintain the forced equilibrium at the reference tension, velocity and thickness values; and (2) a feedback control law for the coiler motor based on measurements of strip tension and coiler angular velocity for coiling of the peeled strip and regulation of strip tension.

Note that the forced equilibrium represents the ideal state of the system which allows for determining the reference values for the states and inputs. Since strip transport systems are operational only under closed-loop control, forced equilibrium at the reference tension and velocity acts as a baseline. The feedforward control component, derived from the governing equations, is designed to maintain the system at this ideal forced equilibrium. It provides the necessary control inputs to achieve the desired tension and velocity under ideal operating conditions, without accounting for disturbances or variations. However, real-world processes are subject to various disturbances and uncertainties. Therefore, the objective of the feedback control mechanism is to make real-time adjustments to correct any deviations from this forced equilibrium state based on real-time monitoring of actual process variables (strip tension and transport velocity). In the following, the necessary feedforward control input and the reference velocity for the forced equilibrium condition are determined. The linearized governing equations for strip velocity and tension errors that are utilized for feedback controller design are also provided.

4.1 Equilibrium control and reference inputs. Let u_{2r} be the control input that maintains the forced equilibrium at reference strip transport velocity v_{2r}, tension T_r, thickness t_r. Since strip with a certain reference thickness t_r is formed at a given reference tension T_r (see Eq. (14)), one has to determine this relationship between T_r and t_r. In this work, an empirical experimental process is employed to determine the relationship between t_r and T_r for different metals, as an analytical model is yet to be developed. In addition, define the following variations: $\widetilde{u}_2(t) := u_2(t) - u_{2r}$ and $\widetilde{v}_2(t) := v_2(t) - v_{2r}$. The coiler dynamics can be written as

$$\frac{J_2}{R_2}(\dot{\widetilde{v}}_2(t) + \dot{v}_{2r}) = -R_2(\widetilde{T}(t) + T_r) - \frac{b_{f2}}{R_2}(\widetilde{v}_2(t) + v_{2r})$$

$$+ n_2(\widetilde{u}_2 + u_{2r}). \tag{23}$$

Under the assumption that the variations $\widetilde{T}, \widetilde{v}_2, \widetilde{u}_2$ and their derivatives are zero at the forced equilibrium, the corresponding equilibrium input is given by

$$u_{2r} = \frac{b_{f2}}{n_2 R_2}v_{2r} + \frac{R_2}{n_2}T_r. \tag{24}$$

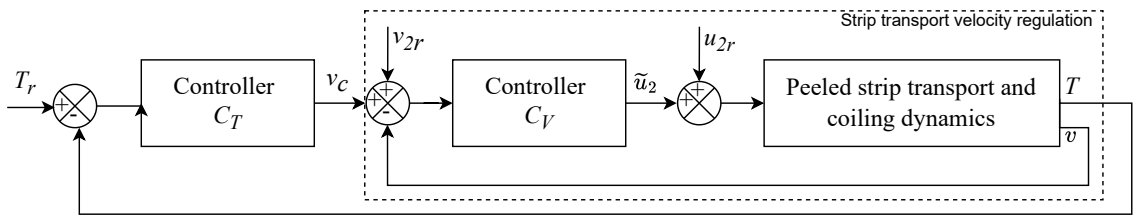

Fig. 5 Cascaded control strategy for peeled strip transport and coiling.

Similarly, the strip transport dynamics is given by

$$\eta(\dot{\widetilde{T}}(t)+\dot{T}_r) = \left(t_r - k\widetilde{T}(t-\tau_2)\right)\left(\widetilde{v}_2(t)+v_{2r}\right) - t_0 v_0$$

$$- v_{2r}k\left(\widetilde{T}(t)-\widetilde{T}(t-\tau_2)\right) - \frac{\eta(\widetilde{T}(t)+T_r)}{L}\left(\widetilde{v}_2(t)+v_{2r}\right), \quad (25)$$

which under forced equilibrium ($\dot{\widetilde{T}} = \widetilde{T} = \dot{\widetilde{v}} = \widetilde{v}_2 = 0$) gives the following relation for the reference velocity v_{2r}

$$v_{2r} = \frac{t_0 v_0}{t_r - T_r/(w_u E)}. \quad (26)$$

Note that the forced equilibrium is valid only under ideal conditions. In practice, there will be dynamic variations due to process and machine induced disturbances, thus, the need for using feedback control to compensate and provide robustness to handle real-world variations and disturbances.

Substituting the reference values for u_{2r} and v_{2r} from equations (24) and (26) into (23) and (25), and simplifying, the following equations for the error dynamics are obtained:

$$\eta\dot{\widetilde{T}}(t) = t_r\widetilde{v}_2(t) - k\widetilde{v}_2(t)\widetilde{T}(t-\tau_2) - v_{2r}k\widetilde{T}(t)$$

$$- \frac{\eta}{L}\left(T_r\widetilde{v}_2(t) + \widetilde{T}(t)\left(\widetilde{v}_2(t)+v_{2r}\right)\right), \quad (27a)$$

$$\frac{J_2}{R_2}\dot{\widetilde{v}}_2(t) = -\frac{b_{f2}}{R_2}\widetilde{v}_2(t) - \widetilde{T}(t)R_2 + n_2\widetilde{u}_2. \quad (27b)$$

Linearizing the strip tension and transport velocity error dynamics equations, by assuming that the product of variations to be negligible, results in the following equations:

$$\dot{\widetilde{T}}(t) = -a_{11}\widetilde{T}(t) + a_{12}\widetilde{v}_2(t), \quad (28a)$$

$$\dot{\widetilde{v}}_2(t) = -a_{21}\widetilde{T}(t) - a_{22}\widetilde{v}_2(t) + b_1\widetilde{u}_2, \quad (28b)$$

where

$$a_{11} = \frac{v_{2r}(\eta+kL)}{\eta L}, \quad a_{12} = \frac{t_r L - \eta T_r}{\eta L},$$

$$a_{21} = \frac{R_2^2}{J_2}, \quad a_{22} = \frac{b_{f2}}{J_2}, \quad b_1 = \frac{n_2 R_2}{J_2}.$$

The above linear state equations and availability of measured strip tension and transport velocity data means that any state feedback controller may be employed for $\tilde{u}_2$. However, this is seldom practiced in the metals industry as a parallel implementation of both the tension and velocity loops is often less robust, since small variations in speed can cause large variations in tension, and vice-versa, due to large elastic modulus for metals strips [42]. In addition, direct measurement of transport velocity at the coil is generally not available and it is common to estimate the transport velocity based on measured angular velocity of the coiler motor and coil diameter estimate based on the nominal strip thickness and angular velocity measurement. In view of these considerations, a cascaded control strategy is often employed which consists of two nested feedback loops: an inner loop for velocity control and an outer loop for tension regulation.

4.2 Feedback control strategy. The structure of the cascaded control strategy is shown in Fig. 5, where the controller output of the outer tension loop provides reference velocity corrections to the inner velocity loop. This dual-loop approach allows for (1) the precise adjustment of strip velocity and tension, (2) incorporation of strip tension feedback to address disturbances that are reflected in the tension signal (as opposed to open loop tension response when employing strip transport velocity regulation only, shown by the dashed line block in Fig. 5), and (3) reduced overall variability and effective response to disturbances. In this paper, as a first step to design a working closed-loop control law for producing metal strips by peeling and coiling, PI controllers are employed for the inner and outer loops. Since R2R machines primarily use rotating machinery, such as rotary motors and rollers, periodic oscillations are dominant in measured variables such as tension and velocity. A proportional controller offers a fast response but often fails to eliminate steady-state errors. Eliminating steady-state error is crucial for producing a strip of consistent thickness and quality, as any error in tension and velocity is reflected as variations in the strip thickness. The integral component in the PI controller addresses accumulated errors, ensuring the system maintains the desired reference values for tension and velocity (i.e., zero steady-state error). Additionally, as discussed in Sec. 5.1, we use a load cell roller to measure roller reaction forces from which the strip tension is calculated. This measurement is subject to high-frequency noise and incorporating a derivative term would amplify this noise. Thus, the following controller transfer functions for the inner loop and outer loop are chosen:

$$C_T(s) = K_{pT} + \frac{K_{iT}}{s}, \quad \text{and} \quad C_V(s) = K_{pV} + \frac{K_{iV}}{s}, \quad (29)$$

where K_{pT}, K_{iT}, K_{pV}, and K_{iV} are the controller gains. Let $\widetilde{U}_2(s)$ and $\widetilde{V}_2(s)$ be the Laplace transforms of $\widetilde{u}_2(t)$ and $\widetilde{v}_2(t)$, respectively. Then, the coiler motor torque input ($\widetilde{U}_2(s)$) is given by

$$\widetilde{U}_2(s) = -C_V(s)\left(\widetilde{V}_2(s) + V_c(s)\right)$$

$$= -C_V(s)\left(\widetilde{V}_2(s) - C_T(s)\widetilde{T}(s)\right). \quad (30)$$

The following closed-loop characteristic equation is obtained by taking the Laplace transform of the linearized error equations (28) and substituting the control input from (30):

$$s^4 + \alpha_3 s^3 + \alpha_2 s^2 + \alpha_1 s + \alpha_0 = 0, \quad (31)$$

where

$$\alpha_0 = K_{iT}K_{iV}a_{12}b_1,$$

$$\alpha_1 = K_{iV}a_{11}b_1 + K_{iT}K_{pV}a_{12}b_1 + K_{iV}K_{pT}a_{12}b_1,$$

$$\alpha_2 = K_{iV}b_1 + a_{11}a_{22} + a_{12}a_{21} + K_{pV}a_{11}b_1 + K_{pT}K_{pV}a_{12}b_1,$$

$$\alpha_3 = a_{11} + a_{22} + K_{pV}b_1.$$

One can choose the control gains for the velocity loop and tension loop controllers to place the roots of the characteristic equation. Theoretical methods for control gain selection such as the Routh-Hurwitz criterion, pole placement and frequency response methods, though insightful for stability and performance analysis, do not directly guide the selection of controller gains in this particular case with non-linear coefficients, since they require iterative approaches and optimization techniques to achieve specific performance criteria. Given these challenges, established practices in R2R manufacturing were utilized for tuning the controller gains. Industrial web tension control systems typically employ a fixed gain PI controller (or a variable gain PI controller for unwind/rewind rollers), with

gains tuned empirically to ensure stable operation under given conditions and material properties (see [20,42]). This empirical tuning is essential due to the variability in operating condition, uncertainties in web material and machine parameters, as well as the need to accommodate system nonlinearities and unmodeled dynamics. Specifically, for the cascaded structure, the tuning process involves adjusting the velocity loop gains (K_{pV}, K_{iV}) first using a simulated load (to mimic load due to strip transport) to achieve desired velocity response and ensure motor stability and zero steady-state error at various reference velocities, and then subsequently tuning the tension loop gains (K_{pT}, K_{iT}) to attain the desired tension performance.

5 EXPERIMENTAL DEMONSTRATION

5.1 Experimental platform. A lab-scale prototype metal peeling system as shown in Fig. 6 was used to implement and test the performance of the proposed control strategy. There are three main elements to this system: (1) peeling of a strip from a disk-shaped feedstock mounted on a lathe spindle; (2) continuous transport of peeled strip to the coiler over several rollers, including a roller mounted on a load cell (load cell roller) which is employed for real-time feedback of strip tension; and (3) a coiling motor connected to the coil roll shaft through a gear transmission.

The peeling experiments were carried out on a flat-bed CNC lathe in a constant feedstock surface velocity ($v_0 = 0.203$ m/s) and depth of cut ($t_0 = 102$ µm) mode. The feedstock material used in the experiments was a 12.7 mm thick low-carbon steel disk (AISI 1018 grade), while the cutting tool was made of tungsten carbide coated with an AlTiN abrasive-resistant coating and had a rake angle (α) of 30°. The cutting velocity and rake angle were chosen to ensure that the strip that forms is continuous and is characterized by uniform shear strain across its cross-section, as the chip formation mode in orthogonal cutting is sensitive to the cutting conditions. For example, higher rake angles are known to promote smooth and continuous strips that are beneficial for strip peeling, whereas combinations of smaller rake angles and high cutting speeds can potentially lead to less desirable chip formation modes such as segmented or discontinuous chips due to strain localization and fracture [43,44]. Note that the strip width is same as the disk feedstock thickness, i.e., $w_u = 12.7$ mm. For strip transport and coiling, a 3-HP capacity, three-phase AC induction motor coupled to a 10:1 gearbox was used to drive the coiling shaft. The real-time control and data acquisition system consists of a motor drive, Programmable Logic Controller (PLC), input/output cards (I/O), and real-time software. The control strategy (Fig. 5) was implemented as four main subprograms: (1) equilibrium inputs (feedforward) evaluator, (2) coil diameter estimator, (3) transport velocity controller, and (4) strip tension controller, which run simultaneously. As noted earlier, real-time tension feedback is provided by an in-line load cell mounted on an idle roller, while an optical encoder mounted on the coiling motor shaft provides real-time angular velocity feedback. This angular velocity feedback, along with the reference strip thickness t_r, was used to continuously estimate the coil radius. The coil radius and angular velocity data together provided an estimate of the coiler surface velocity. Note that in the absence of any errors in the coil radius, this velocity is same as the strip transport velocity v_2.

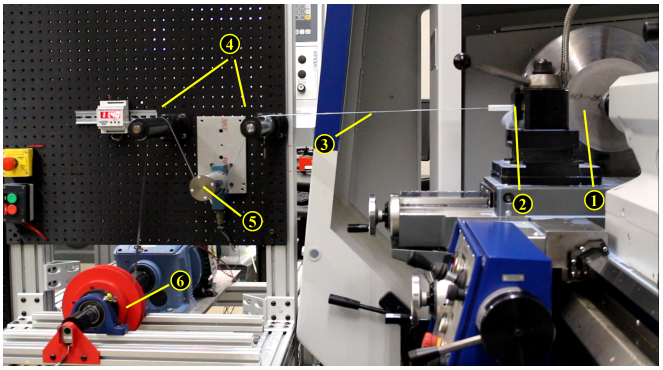

Fig. 6 Experimental platform used for peeling experiments: 1: feedstock, 2: cutting tool; 3: strip, 4: idle rollers, 5: load cell roller, 6: coiler.

Two sets of experiments were carried out and compared: (1) velocity control experiments where the objective was to maintain a constant coiler surface velocity (via control of angular velocity) without a tension loop, and (2) tension control experiments involving a cascaded control strategy that adjusts the coiler surface velocity to maintain a desired tension based on real-time tension feedback from the load cell. Established practices in web handling and conventional sheet processing suggest an average tension of less than 10% of the material's yield strength [45]. However, in the case of peeling, a tensile stress of at least ~ 15% of the yield strength was found to be necessary to produce a malleable strip with reduced edge waviness and out-of-plane curvature. Thus, in tension control experiments, the strip reference tension (T_r) was set at 155 N. The reference transport velocity (v_{2r}) in both the velocity and tension control experiments was similar, 0.087 m/s and 0.094 m/s, respectively. While employing only velocity regulation (shown by the dashed block in Fig. 5), T_r was not set, however, tension feedback measurement from the load cell was recorded. The following sampling times were used in the control implementation: velocity loop: 20 ms; tension loop: 100 ms; coil diameter updates: 50 ms; and feedforward input updates: 500 ms. The first 50 seconds of the data reported in the results represent the transient response due to coiling initiation, i.e., the response during the time between coiling the initial peeled strip with a slack and achieving steady-state tension and velocity.

5.2 Results and discussion. This section presents results from peeling experiments undertaken to evaluate the performance of the controllers in regulating strip tension and transport velocity. Figures 7 and 8 show the evolution of errors in strip tension and coiler surface velocity in both the control strategies. Data is shown for a ~ 4 minute time period, which corresponds to a coil length of about 25 m. In these plots, $\widehat{T}$ and $\widehat{v}_2$ represent the non-dimensional errors in strip tension and coiler surface velocity given by

$$\widehat{T} = \frac{\widetilde{T}}{T_r}, \quad \widehat{v}_2 = \frac{\widetilde{v}_2}{v_{2r}}. \tag{32}$$

In the velocity control experiments (without tension loop), the average steady-state tension of the recorded tension measurement was used instead of T_r to compute $\widehat{T}$. From the velocity control experiment in Fig. 7, it can be seen that the coiler surface velocity was regulated around the desired reference v_{2r} value with a steady-state mean error and standard deviation of 1% and 0.8%, respectively. Although velocity regulation was efficient, tension variations were somewhat large, about ± 25% from the mean tension value during steady-state operation. As a reference, the mean tension in this case is 150 N, which corresponds to a tensile stress σ_s of 60 MPa; therefore, 25% tension variation represents a variation of 15 MPa or about 4% of the strip's shear flow stress. While it is difficult to pinpoint the origin of these tension variations, they are likely a result of errors in the estimated coil radius. In this regard, real-time measurement of coil radius, for example using a laser sensor, is expected to further improve the tension error performance.

Figure 8 presents data from a tension control experiment. It is seen that tension error performance in this case is superior when compared to implementation without the tension loop, with a steady-state mean tension error of 2% from the reference, a standard deviation of 4%, and a maximum deviation of ± 13% from the mean value. The corresponding velocity error performance was similar to that in Fig. 7. These observations suggest that in the absence of direct strip transport velocity feedback, active control of strip tension

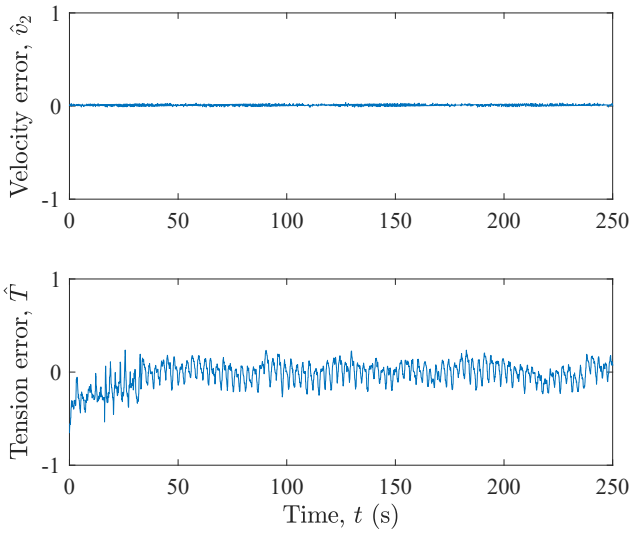

Fig. 7 Strip transport velocity and tension error profile in a velocity control experiment (without tension feedback).

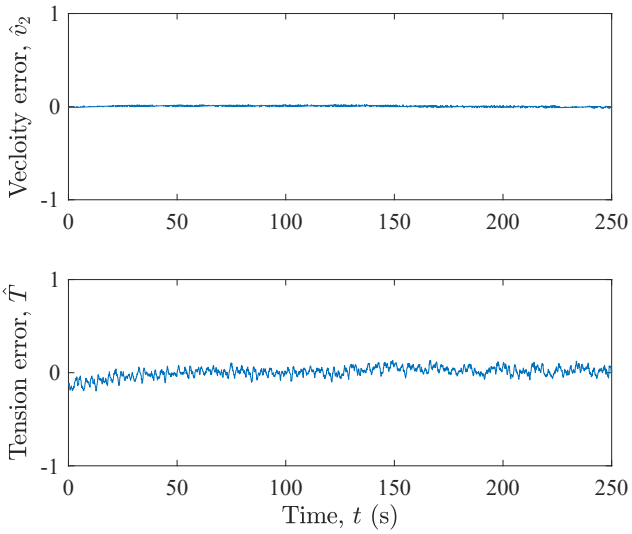

Fig. 8 Strip transport velocity and tension error profile in a tension control experiment (with tension feedback).

provides better performance over controlling coiler surface velocity alone without tension feedback. To understand the strip thickness characteristics of coils, strip thickness cross-sections taken from different coil lengths were investigated using optical microscopy. In these measurements, slightly larger thickness variations were observed in the unregulated tension case (standard deviation of 8%) when compared to the regulated tension case (standard deviation of 3.8%). These observations are consistent with the larger tension variations seen in Fig. 7 vs. Fig. 8. Another important benefit of incorporating tension feedback is that it provides a means to compensate for machine disturbances and process variations (both sudden and slowly varying) since these are reflected in the tension feedback signal. Experiments were conducted to evaluate this aspect by purposefully inducing disturbances through small step changes in the feedstock surface velocity (v_0), see Fig. 9. The sharp tension drop at the 200 second mark in the figure is due to step perturbation of 5% increase in v_0, while that at the 300 second mark corresponds to a step perturbation of $1.05v_0$ to $0.95v_0$ (~10% decrease). From the tension plot, it is evident that tension is regulated back to the set point value of 150 N in both the cases. These observations confirm that the controller regulates tension at the desired reference value despite disturbances, validating the feedback controller's capability to handle dynamic variations in the process and maintaining consistent strip quality. The ability to regulate strip tension at different reference values is shown in Fig. 10, which shows tension data from three different experiments carried out with different tension set points of 155 N, 200 N and 245 N (and reference velocities of 0.094 m/s, 0.103 m/s and 0.111 m/s, respectively). In all cases, tension converges to the desired reference values with a mean steady-state error under 3%, and a post-settling standard deviation of about 5%. Similarly, velocity in all cases converged to the desired reference with steady-state mean error and standard deviation well within 1%. These results indicate that the dynamic model effectively captures the essential characteristics of the strip transport process, as well as the contribution of the feedforward control input to drive the system to the desired state.

Experiments performed under various levels of strip tension during peeling have also revealed that the geometric attributes and material properties of the peeled strip are significantly influenced by the magnitude of tension. For example, Fig. 11 depicts the effect of applied tension on strip edge waviness and curvature. It is seen that a higher tensile stress (σ_s) has a positive impact on strip quality in terms of reducing both edge waviness and out-of-plane curvature. Note that due to strip thickness dependence on tension in peeling, isolation of tension effects from thickness effects requires simultaneous feedback and control of the feedstock velocity (v_0). Such experiments to investigate tension effects on strip quality are planned in the future.

6 CONCLUSIONS AND FUTURE WORK

This paper modeled the strip transport behavior in metal peeling and developed a control strategy for the transport of peeled strip from the cutting edge to the coiler. In particular, governing equations for strip tension and transport velocity that incorporate the interaction between between applied strip tension and thickness were developed. As a first step, an efficient and yet simple cascaded control strategy was proposed based on these equations to regulate strip tension. An experimental platform was developed and peeling experiments were conducted employing the proposed tension control strategy. The experimental results confirm the efficacy of the proposed control strategy in terms of achieving the desired strip tension, velocity and thickness values and maintaining stability with minimal error. The robustness of the system in the presence of large machine disturbances and process variations was also verified. Taken together, the work demonstrated the need for regulating strip tension in peeling and its positive impact on strip quality.

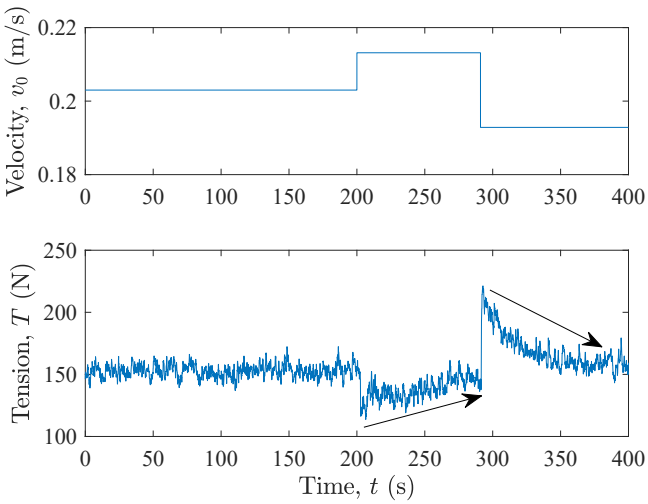

Fig. 9 Tension regulation under induced disturbances in the feedstock surface velocity (v_0).

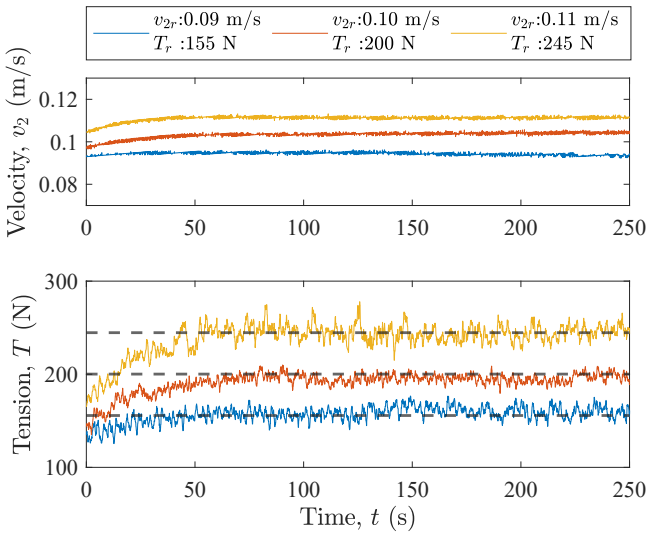

Fig. 10 Velocity and tension plots showing the ability to achieve and maintain constant reference values under different set-point conditions.

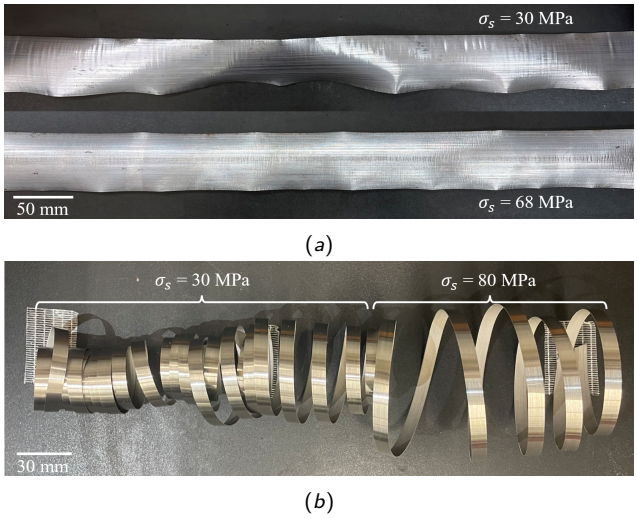

Fig. 11 Effect of tension on (a) edge waviness (low-carbon steel, 50 mm width), and (b) out-of-plane curvature (stainless steel, 9.5 mm width). Stainless steel was chosen for the latter demonstration because of its propensity to form a highly curled strip.

Potential future work includes scaling to larger widths, thicknesses and transport velocities and development of model-based controllers to aid controlled strip production under a wide variety of conditions, including zero-speed splicing using an accumulator and ramp up from zero speed to full speed for the coiler. It is expected that with larger widths, both machine induced disturbances and peeled strip shape irregularities (such as flatness and edge waviness) may arise; thus, model-based controllers that can efficiently regulate strip tension and transport velocity under varying dynamic conditions will be needed. Specifically, robust and adaptive controllers that incorporate a detailed dynamic process model, including nonlinearities in the governing equations, to account for uncertainty in the process as well as system parameters will be explored. This is expected to eliminate the need for re-tuning under different operating conditions or material properties, thereby enhancing the control system's robustness and adaptability. Further, the shape irregularities that are expected to arise during peeling of wider strips may require additional model development and control design, including regulation of the strip's lateral position during transport and coiling. The strip transport model in this paper assumed an ideal rectangular cross-section of the peeled strip and does not directly account for edge waviness and out-of-plane curvature. Future work could involve modifying the governing equations for strip transport both in the span and within the coil to account for these non-ideal conditions. The current feedback-feedforward controller structure within the cascaded control strategy allows for feedforward compensation to include terms that predict and counteract edge waviness and curvature based on current and past measurements. For example, see [46] for modeling and control in the presence of non-ideal rollers. Other refinements could include replacing fixed-gain PI controllers with adaptive control algorithms that adjust parameters in real-time based on current system performance, and incorporation of sensors specifically designed to detect edge waviness and out-of-plane curvature (e.g., laser displacement sensors or high-resolution cameras) to provide detailed feedback to the control system for more precise control actions.

Acknowledgment

The authors thank Breakthrough Energy (through the Fellows Program) and the US National Science Foundation (through grant no. CMMI - 2102030) for sponsoring this research, and Boliang Meng, Ravi Srivatsa, Parth Dave, and Ashish Devkota of Texas A&M University for their help in conducting the experiments.

References

[1] Semiatin, S., ed., 2005, *ASM Handbook volume 14A: Metalworking: Bulk forming*, ASM International, Materials Park, OH.
[2] Roberts, W., 1983, *Hot rolling of steel*, CRC Press.
[3] Fruehan, R., Fortini, O., Paxton, H., and Brindle, R., 2000, "Theoretical minimum energies to produce steel for selected conditions," US OSTI Technical Report, doi: 10.2172/1216249.
[4] Junker, O., 1929, "US Patent 1701889 - Method for manufacturing metal sheets and strips," .
[5] Shaw, M. and Hoshi, T., 1976, "A new method of manufacturing wire," *Proceedings of the Sixteenth International Machine Tool Design and Research Conference*, Springer, pp. 459–465, doi: 10.1007/978-1-349-81544-9_61.
[6] Middlemiss, A., Hague, D., and Gleave, M., 1982, "Strip production by peeling," Metals Technology, **9**(1), pp. 413–418.
[7] Brown, R., 1989, "Strip fabrication using peeling techniques," Materials and Manufacturing Processes, **4**(4), pp. 467–481.
[8] Vigor, C. W. and Leibring, W., 1973, "Metal peeling for production of stainless steel foil for gas turbine regenerators," SAE Transactions, **82**, pp. 435–440.
[9] Middlemiss, A. and Malkani, D. T., 1977, "US Patent 4213231A - Manufacture of metal strip," .
[10] Childs, T. and Walters, M., 1986, "Machining with applied chip tension—Part II: Experiments," International Journal of Mechanical Sciences, **28**(11), pp. 769–779.
[11] De Chiffre, L., 1983, "Extrusion cutting of brass strips," International Journal of Machine Tool Design and Research, **23**(2), pp. 141–151.
[12] Moscoso, W., 2008, "Severe plastic deformation and nanostructured materials by large strain extrusion machining," Ph.D. thesis, Purdue University.
[13] Sagapuram, D., Efe, M., Moscoso, W., Chandrasekar, S., and Trumble, K. P., 2013, "Controlling texture in magnesium alloy sheet by shear-based deformation processing," Acta Materialia, **61**(18), pp. 6843–6856.
[14] Sagapuram, D., Kustas, A., Dale Compton, W., Tumble, K., and Chandrasekar, S., 2015, "Direct single-stage processing of lightweight alloys into sheet by hybrid cutting-extrusion," ASME Journal of Manufacturing Science and Engineering, **137**(5), p. 051002.
[15] Zhang, F. and De Chiffre, L., 1987, "Effect of applied tension on quality of brass strip manufactured by extrusion cutting," CIRP Annals, **36**(1), pp. 53–56.
[16] King, D., 1969, "The mathematical model of a newspaper press," Newspaper Techniques, **1**, pp. 3–7.
[17] Brandenburg, G., 1976, "New mathematical models for web tension and register error," *3rd International IFAC Conference on Instrumentation and Automation in the Paper*, Vol. 1, Rubber and Plastics Industries.
[18] Whitworth, D. P. D. and Harrison, M., 1983, "Tension variations in pliable material in production machinery," Applied Mathematical Modelling, **7**(3), pp. 189–196.
[19] Young, G. E. and Reid, K. N., 1993, "Lateral and longitudinal dynamic behavior and control of moving webs," ASME Journal of Dynamic Systems, Measurement, and Control, **115**(2B), pp. 309–317.
[20] Pagilla, P. R., Siraskar, N. B., and Dwivedula, R. V., 2006, "Decentralized control of web processing lines," IEEE Transactions on Control Systems Technology, **15**(1), pp. 106–117.
[21] Seshadri, A. and Pagilla, P. R., 2009, "Optimal web guiding," ASME Journal of Dynamic Systems, Measurement, and Control, **132**(1), p. 011006.

[22] Perduková, D., Fedor, P., Fedák, V., and Padmanaban, S., 2019, "Lyapunov based reference model of tension control in a continuous strip processing line with multi-motor drive," Electronics, **8**(1), p. 60.
[23] Hu, Y., Sun, J., Chen, S. Z., Zhang, X., Peng, W., and Zhang, D., 2019, "Optimal control of tension and thickness for tandem cold rolling process based on receding horizon control," Ironmaking & Steelmaking.
[24] Akil, A. and Rabbah, N., 2024, "A nonlinear design method of robust PI control by using adaptive backstepping control for web winding system of reversible cold rolling mill," The International Journal of Advanced Manufacturing Technology, pp. 1–16.
[25] Liu, L., Shao, N., Lin, M., and Fang, Y., 2019, "Hamilton-based adaptive robust control for the speed and tension system of reversible cold strip rolling mill," International Journal of Adaptive Control and Signal Processing, **33**(4), pp. 626–643.
[26] Gaber, A., Elnaggar, M., and Fattah, H. A., 2022, "Looper and tension control in hot strip finishing mills based on different control approaches," Journal of Engineering and Applied Science, **69**(1), p. 100.
[27] Shaw, M., 1984, *Metal cutting principles*, Clarendon Press, Oxford Science Publications.
[28] Sagapuram, D., Udupa, A., Viswanathan, K., Mann, J. B., M'Saoubi, R., Sugihara, T., and Chandrasekar, S., 2020, "On the cutting of metals: A mechanics viewpoint," ASME Journal of Manufacturing Science and Engineering, **142**(11), p. 110808.
[29] Merchant, M. E., 1945, "Mechanics of the metal cutting process. I. Orthogonal cutting and a type 2 chip," Journal of Applied Physics, **16**(5), pp. 267–275.
[30] Lee, E. H. and Shaffer, B. W., 2021, "The theory of plasticity applied to a problem of machining," ASME Journal of Applied Mechanics, **18**(4), pp. 405–413.
[31] Oxley, P. L. B., 1989, *The mechanics of machining: An analytical approach to assessing machinability*, Ellis Horwood.
[32] Nakayama, K., 1964, "Effects of tension applied to chip during metal-cutting: Chip-pulling cutting," Bulletin of the Faculty of Engineering, Yokohama National University, **13**, pp. 7–16.
[33] Walters, M. and Childs, T., 1984, "The strip peeling of steels," *Proceedings of the Twenty-Fourth International Machine Tool Design and Research Conference*, Springer, pp. 127–134, doi: 10.1007/978-1-349-81247-9_18.
[34] Hill, R., 1954, "The mechanics of machining: A new approach," Journal of the Mechanics and Physics of Solids, **3**(1), pp. 47–53.
[35] Kobayashi, S. and Thomsen, E. G., 1962, "Metal-cutting analysis—I: Re-evaluation and new method of presentation of theories," ASME Journal of Engineering for Industry, **84**(1), pp. 63–70.
[36] Armarego, E. and Brown, R., 1969, *The machining of metals*, Prentice-Hall, Inc.
[37] Dewhurst, P., 1978, "On the non-uniqueness of the machining process," Proceedings of the Royal Society of London. A. Mathematical and Physical Sciences, **360**(1703), pp. 587–610.
[38] Finnie, I. and Wolak, J., 1963, "Use of chip tension to obtain a stress-strain curve from metal mutting tests," ASME Journal of Engineering for Industry, **85**(4), pp. 351–355.
[39] Lu, Y. and Pagilla, P. R., 2013, "Modeling the effects of heat transfer processes on material strain and tension in roll to roll manufacturing," *ASME Dynamic Systems and Control Conference*, Vol. 56147, p. V003T48A004, doi: 10.1115/DSCC2013-4075.
[40] Jabbar, K. A. and Pagilla, P. R., 2018, "Modeling and analysis of web span tension dynamics considering thermal and viscoelastic effects in roll-to-roll manufacturing," ASME Journal of Manufacturing Science and Engineering, **140**(5), p. 051005.
[41] Pagilla, P. R., King, E. O., Dreinhoefer, L. H., and Garimella, S. S., 2000, "Robust observer-based control of an aluminum strip processing line," IEEE Transactions on Industry Applications, **36**(3), pp. 865–870.
[42] Raul, P. R., 2015, "Design and analysis of feedback and feedforward control systems for web tension in roll-to-roll manufacturing," Ph.D. thesis, Oklahoma State University.
[43] Viswanathan, K., Yadav, S., and Sagapuram, D., 2020, "Shear bands in materials processing: Understanding the mechanics of flow localization from Zener's time to the present," ASME Applied Mechanics Reviews, **72**(6), p. 060802.
[44] Yadav, S., Chawla, H., and Sagapuram, D., 2024, "In situ observations of shear localization and fracture in machining," *Proceedings of the ASME 2024 International Manufacturing Science and Engineering Conference*, in press.
[45] Roisum, D. R., Walker, T. J., and Jones, D. P., 2021, *The web handling handbook*, DEStech Publications, Incorporated.
[46] Branca, C., Pagilla, P. R., and Reid, K. N., 2013, "Governing equations for web tension and web velocity in the presence of nonideal rollers," ASME Journal of Dynamic Systems, Measurement, and Control, **135**(1), p. 011018.